Clin Neuroradiol (2020) 30:569–579
https://doi.org/10.1007/s00062-019-00805-0

ORIGINAL ARTICLE

Microstructural White Matter Alterations in Mild Cognitive Impairment and Alzheimer's Disease

Study Based on Neurite Orientation Dispersion and Density Imaging (NODDI)

Xiuwei Fu[1] · Susan Shrestha[1] · Man Sun[2] · Qiaoling Wu[3] · Yuan Luo[1] · Xianchang Zhang[4] · Jianzhong Yin[5] · Hongyan Ni[5]

Received: 21 February 2019 / Accepted: 21 May 2019 / Published online: 7 June 2019

Abstract

Purpose To investigate microstructural alterations in white matter in mild cognitive impairment (MCI) and Alzheimer's disease (AD) using neurite orientation dispersion and density imaging (NODDI) and to assess the potential diagnostic performance of NODDI-derived parameters.

Methods In this study 14 MCI patients, 14 AD patients, and 14 healthy controls (HC) were recruited. The diffusion tensor imaging(DTI)-derived fractional anisotropy (FA) and NODDI-derived neurite density index (NDI), orientation dispersion index (ODI), and volume fraction of isotropic water molecules (Viso) were calculated from the diffusion data. The tract-based spatial statistics (TBSS) method was used for statistical analysis with one-way ANOVA. The correlations between the parameter values and mini-mental state examination (MMSE) and Montreal cognitive assessment (MoCA) scores were examined. A receiver operating characteristic (ROC) curve was conducted to assess the diagnostic performance of different parameters.

Results Compared with the HC group, the NDI and ODI values decreased significantly and the Viso values were significantly increased in the MCI and AD groups ($p<0.01$, threshold-free cluster enhancement (TFCE)-corrected); however, there were no significant differences in FA values in the MCI group. The NDI, ODI, and Viso values of multiple fibers were significantly correlated with MMSE and MoCA scores. For the diagnosis of AD, the area under the ROC curve (AUC) for the NDI value of the splenium of corpus callosum was larger than the FA value (AUC = 0.885, 0.714, $p=0.042$). The AUC of the Viso value of the right cerebral peduncle was larger than FA value (AUC = 0.934, 0.531, $p=0.004$).

Conclusion The NDI is more sensitive to white matter microstructural changes than FA and NODDI could be superior to DTI in the diagnosis of AD.

Keywords Neurite density · Orientation dispersion · Isotropic water molecule · Fractional anisotropy · Diffusion tensor imaging

Electronic supplementary material The online version of this article (https://doi.org/10.1007/s00062-019-00805-0) contains supplementary material, which is available to authorized users.

✉ Hongyan Ni
nihyan@sina.com

[1] Department of Radiology, First Central Clinical College, Tianjin Medical University, Tianjin, China

[2] Department of Radiology, Tianjin Hospital of Tianjin, Tianjin, China

[3] Tianjin University of Traditional Chinese Medicine, Tianjin, China

[4] MR Collaboration, Siemens Healthcare Ltd., Beijing, China

[5] Department of Radiology, Tianjin First Central Hospital, 24 Fukang Road, Nankai District, 300192 Tianjin, China

Introduction

Alzheimer's disease (AD) is a neurodegenerative disorder and is the most common type of dementia. Many researchers and clinicians hypothesize that the pathophysiology of AD can be explained by extracellular amyloid beta (Aβ) deposits that precipitate senile plaques and intracellular deposits of abnormal tau protein that precipitate neurofibrillary tangles [1]; however, previous studies based on diffusion tensor imaging (DTI) have shown that white matter damage is also present in the early stages of AD and thus may also represent the pathophysiology of AD [2, 3]. Furthermore, it is speculated that the beginnings of these white matter changes may also be present in mild cognitive impairment (MCI), which has an annual conversion rate to AD of 5–15%, much greater than that of healthy elderly people [4]; however, changes in fractional anisotropy (FA), a parameter derived from DTI, can reflect changes in the integrity of the myelin sheath, the density and diameter of the axons and fiber orientation or partial volume effects [5]. Therefore, DTI lacks the specificity for characterizing the possible subtle white matter changes that may occur in patients with MCI before they convert to AD.

Neurite orientation dispersion and density imaging (NODDI) utilizes a multicompartment diffusion model based on the differences between water molecule diffusion in intracellular, extracellular and cerebrospinal fluid (CSF) compartments. It is a promising technique for distinguishing between three different specific microstructural tissue features: intraneurite diffusion, extraneurite diffusion, and the volume fraction within a voxel occupied by isotropic water diffusion [6]. Based on three different compartments, NODDI generates three important parameters, namely neurite density index (NDI), orientation dispersion index (ODI), and the volume fraction of isotropic water molecules (Viso). The NDI represents the volume fraction of neurites in the intraneurite space, ODI evaluates the characteristics of neurite angular variation in the extraneurite space and reflects the changes of fiber orientations in the white matter and Viso represents the volume fraction of water molecules that can diffuse freely like CSF within the voxel [6, 7]. The parameters assessed by NODDI, including neurite density and fiber orientation dispersion, influence the FA value. Thus, NODDI may be able to more accurately evaluate microstructural alterations than FA. Furthermore, it has been demonstrated that the neurite density and orientation dispersion measured by NODDI have good agreement with results of histological measurements in mouse brain and patients with multiple sclerosis [8–10]. The purpose of this study was to investigate microstructural white matter alterations in patients with MCI and AD as detected by NODDI and whether NODDI-derived parameters have the potential to be used diagnostically for MCI and AD.

Material and Methods

Subjects

This study was approved by the local institutional review board. Informed consent was obtained from all subjects and AD and MCI patients were selected from memory clinics from March 2016 to October 2017. Healthy controls (HC) were recruited from the local community and were selected so that they would be matched to the AD and MCI patients by age, gender, and years of education. Inclusion criteria for the AD patients were: (1) meeting the National Institute of Neurological and Communicative Disorders and Stroke and the Alzheimer's Disease and Related Disorders Association (NINCDS-ADRDA) diagnostic criteria for probable AD, (2) mini-mental state examination (MMSE) score $\leq$17 if illiterate, $\leq$20 if subjects did not complete any education beyond primary school, $\leq$24 if subjects completed middle school and above, (3) Montreal cognitive assessment (MoCA)$<$26 and (4) clinical dementia rate (CDR) score$=$1. Inclusion criteria for MCI patients were: (1) meeting the Petersen criteria, namely subjective cognitive decline and confirmed by the informed persons, evidence of cognitive impairment in a single or multiple cognitive domains, preservation of independent daily life abilities and do not meet the diagnostic criteria for dementia [11, 12], (2) MMSE$>$24, (3) MoCA$<$26, (4) CDR score$=$0.5 and (5) still meet the MCI diagnostic criteria after 8–10 months of follow-up. Inclusion criteria for HC were: (1) no evidence of cognitive impairment, (2) MMSE$\geq$27, (3) MoCA$\geq$26 and (4) CDR score$=$0. The exclusion criteria for all subjects were: (1) severe cerebrovascular disease, (2) severe white matter hyperintensity, (3) a history of a psychiatric disorder or severe trauma, (4) a history of medication that affects cognition and (5) left-handedness. Ultimately 14 subjects were enrolled in each of the 3 groups (HC, MCI, and AD) with a total of 42 subjects overall.

Image Acquisition

All MR data were acquired on a 3T MAGNETOM Trio, A Tim System (Siemens Healthcare, Erlangen, Germany) with a 32-channel head coil. All subjects underwent MRI scans with a magnetization prepared rapid acquisition gradient echo (MPRAGE) sequence and an echo planar imaging (EPI) diffusion sequence appropriate for DTI and NODDI models. Diffusion-weighted images were collected using a prototype multi-band EPI sequence with the following parameters: TR/TE$=$4600/95 ms, FOV$=$220 mm$\times$220 mm, matrix$=$110$\times$110, voxel$=$2 mm$\times$2 mm$\times$2 mm, slices$=$70, b$=$0/1000/2000 s/mm^2, directions$=$64, multi-band acceleration factor$=$2, acquisition time$=$10 min 39 s. The

Table 1 Demographic and neuropsychological data analyses

	AD ($n=14$)	MCI ($n=14$)	HC ($n=14$)	p-value
Gender (M/F)	14 (8/6)	14 (6/8)	14 (7/7)	0.751
Age (years)	62.29 ± 8.13	65.21 ± 9.92	62.50 ± 4.15	0.545
Education (years)	12(8.75 ~ 15.00)	12(9.00 ~ 15.00)	12(8.75 ~ 12.00)	0.629
MMSE	14.36 ± 4.70[ab]	24.57 ± 2.06[b]	29.14 ± 0.86	<0.001
MoCA	9.21 ± 4.15[ab]	20.29 ± 2.70[b]	27.79 ± 1.12	<0.001

A χ^2-test was performed for the gender comparison
A one-way ANOVA was used to compare age, MMSE, and MoCA scores; Bonferroni corrections were used in the post hoc test
A Kruskal–Wallis test was used to compare years of education; the results are presented as median (lower quartile ~ upper quartile)
MMSE mini-mental state examination, *MoCA* Montreal cognitive assessment, *AD* Alzheimer's disease, *MCI* mild cognitive impairment, *HC* healthy control, *m* male, *f* female, *ANOVA* analysis of variance
[a]Significantly different compared with the MCI group
[b]Significantly different compared with the HC group

parameters for the MPRAGE sequence were as follows: TR/TE = 1900/2.5 ms, flip angle = 9°, slices = 176, FOV = 256 mm × 256 mm, voxel = 1 mm × 1 mm × 1 mm. Additionally, regular MRI including T2-weighted images (T2WI) and fluid attenuated inversion recovery (FLAIR) were also acquired. Combined with MPRAGE, they were used to exclude cerebrovascular disease, white matter hyperintensity, and other brain lesions.

MRI Data Processing

The diffusion MRI data were processed using the following procedure: 1) the images were converted from Digital Imaging and Communications in Medicine (DICOM) to Neuroimaging Informatics Technology Initiative (NIFTI) format, 2) for quality assurance, two radiologists independently inspected the data for motion or distortion artifacts but did not exclude any of the images, 3) head motion-related artifacts and image distortion due to eddy currents were corrected using the "eddy current correction" tool in FSL toolbox (Oxford Centre for Functional MRI of the Brain; http://fsl.fmrib.ox.ac.uk/fsl/fslwiki/). The DTI parameter FA was calculated using DTIFIT tools in FSL. After extraction of non-brain tissue using Brain Extraction Tool (BET) in FSL, a brain mask was derived to define the regions of NODDI processing using the NODDI_toolbox (www.nitrc.org/projects/noddi_toolbox) in Matlab2012b (Mathworks, Natick, MA, USA). The WatsonSHStickTortIsoV_B0 model was applied to calculate NODDI parameters (NDI, ODI, and Viso) [6].

The tract-based spatial statistics (TBSS) analysis was performed on all parameter maps for statistical analysis. All subjects' images were nonlinearly registered to the FMRIB58_FA template in the Montreal Neurological Institute (MNI) standard space. All the aligned images were averaged, skeletonized and average skeleton maps were generated. Based on the parameter maps that were normalized to the MNI space, the DPABI (http://rfmri.org/dpabi) software package was used to extract the parameter values in each region of interest using the Johns Hopkins University (JHU)-WhiteMatter-labels as masks.

Statistical Analysis

The demographic data and MMSE and MoCA scores of all subjects were statistically analyzed using SPSS 22.0 (IBM Corp., Armonk, NY, USA). Quantitative data with normal distributions were analyzed using one-way ANOVA and the Bonferroni test was used as a post hoc analysis. Nonparametric tests were used for data without normal distributions. The genders of the three groups were analyzed using a χ^2-test. For the TBSS analysis, a statistical matrix of one-way ANOVA was established using a general linear model in FSL and age was used as a covariate. To explore group differences, nonparametric permutation tests with 5000 random permutations were performed by using the randomize command, threshold-free cluster enhancement (TFCE) was used for multiple comparison correction. The final results were overlaid on JHU-WhiteMatter-labels templates to localize the significant clusters in the MNI standard space. The correlations between parameter values in the fibers with MMSE and MoCA scores were analyzed. Spearman correlation analyses were used for data without normal distributions. A receiver operating characteristic (ROC) curve was used to evaluate the diagnostic performance of different parameters.

Results

Demographic data and Neuropsychological Scores

Demographic data and neuropsychological score results are shown in Table 1. There were no significant differences in gender ($p=0.751$), age ($p=0.545$) and years of education ($p=0.629$) between the AD, MCI, and HC groups.

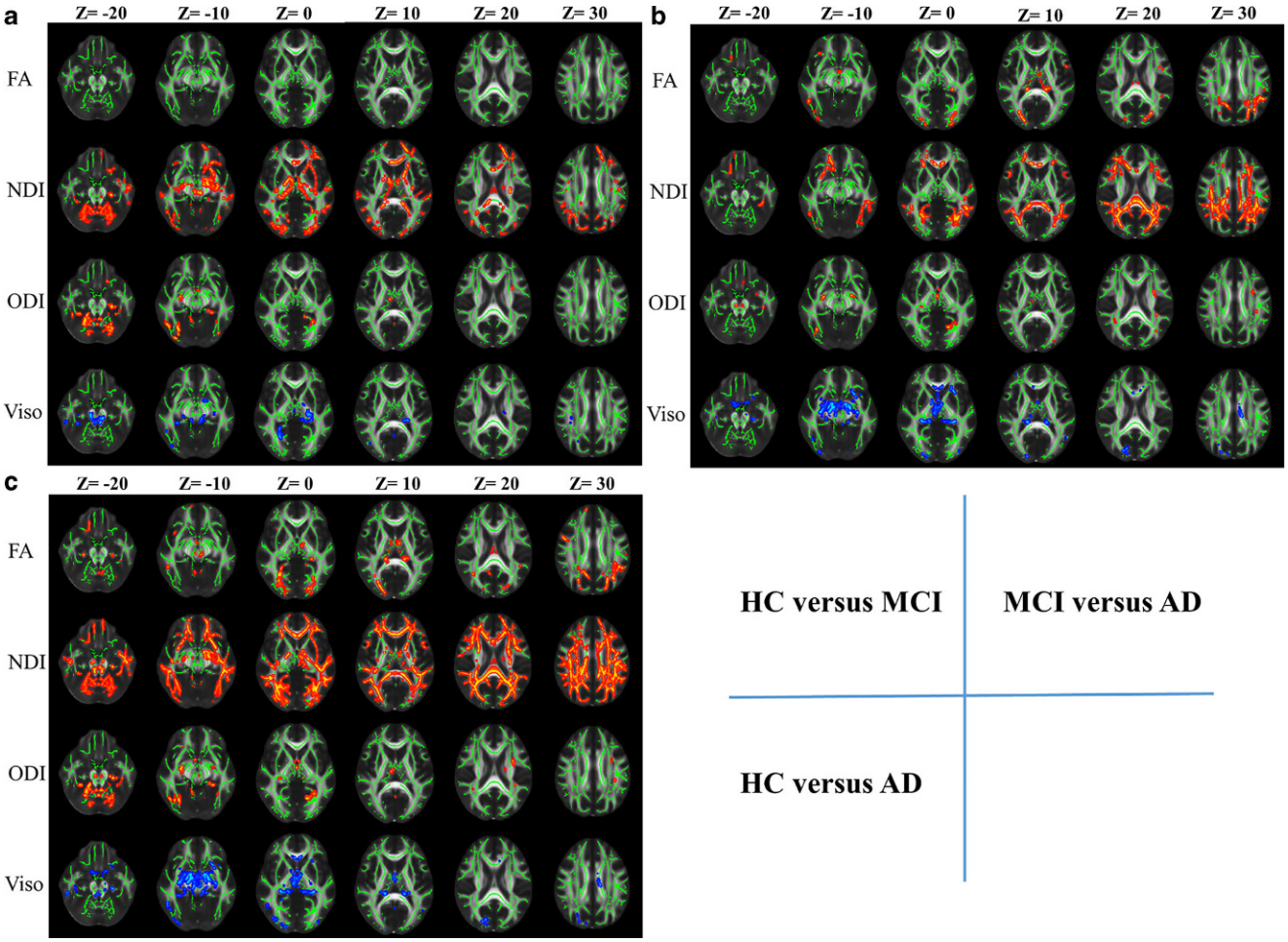

Fig. 1 **a**, **b**, and **c** are the results of comparisons between HC and MCI, MCI and AD, and HC and AD, respectively. *Green* represents the FA skeleton overlaid on the FMRIB58_FA template. *Red-yellow* indicates the brain structures with significantly decreased parameter values in the MCI and AD groups ($p < 0.01$, TFCE-corrected). *Blue* indicates the brain structures with significantly increased parameter values in the MCI and AD groups ($p < 0.01$, TFCE-corrected). *MCI* mild cognitive impairment, *HC* healthy control, *FA* fractional anisotropy, *NDI* neurite density index, *ODI* orientation dispersion index, *Viso* volume fraction of isotropic water molecules, *AD* Alzheimer's disease

There were significant differences in MMSE ($p < 0.001$) and MoCA scores ($p < 0.001$) between the three groups.

FA and NODDI Parameters

For the FA values, there was no significant difference between the HC and MCI groups at the significant threshold of $p < 0.01$ (Fig. 1a); however, the NDI values of the white matter, including the bilateral superior longitudinal fasciculus, the splenium of the corpus callosum, and the left uncinate fasciculus, were significantly lower in the MCI group compared to the HC group, ($p < 0.01$, TFCE-corrected). The brain areas with significantly lower NDI values were mainly located in the middle and lower parts of the brain in the MCI group. The ODI values were significantly lower in the left cingulum, bilateral superior longitudinal fasciculus, and bilateral corticospinal tract of the MCI group compared to the HC group ($p < 0.01$, TFCE-corrected). The Viso values were significantly higher in the bilateral cerebral peduncle, right cingulum, and right superior longitudinal fasciculus of the MCI group compared to the HC group ($p < 0.01$, TFCE-corrected) (Fig. 1a; Table 2).

Compared with the MCI group, the FA values of the white matter in the bilateral superior longitudinal fasciculus and left corticospinal tract were significantly lower in the AD group ($p < 0.01$, TFCE-corrected). Compared to the MCI group, the NDI values for the bilateral superior longitudinal fasciculus, the right cingulum, and the splenium of the corpus callosum were significantly lower in the AD group ($p < 0.01$, TFCE-corrected). The brain areas with significantly decreased NDI values were mainly located in the middle and upper parts of brain in the AD group. The ODI values for the bilateral superior longitudinal fasciculus and left cingulum were significantly lower in the AD group ($p < 0.01$, TFCE-corrected). The Viso values for the bilateral cerebral peduncle, left cingulum, and right superior

Table 2 White matter structures with reduced NDI and ODI values and increased Viso values in the MCI group as compared to healthy controls

Parameters	White matter structures	Side	MNI coordinates			*p*-value
			X	Y	Z	
NDI	Superior longitudinal fasciculus	L	–46	–21	–18	0.008
	Splenium of corpus callosum	–	10	–40	18	0.004
	Superior longitudinal fasciculus	R	30	–72	–7	0.004
	Anterior corona radiata	L	–22	19	12	0.006
	External capsule	L	–34	–3	–4	0.006
	Posterior limb of internal capsule	L	–19	–6	11	0.003
	Genu of corpus callosum	–	–10	29	–4	0.006
	Body of corpus callosum	–	–7	19	19	0.006
	Uncinate fasciculus	L	–35	0	–19	0.005
	Anterior limb of internal capsule	L	–19	12	11	0.004
ODI	Cingulum	L	–24	–21	–24	0.003
	Superior longitudinal fasciculus	R	49	–18	–28	0.001
	Superior longitudinal fasciculus	L	–31	4	18	0.001
	Corticospinal tract	L	–6	–29	–24	0.005
	Corticospinal tract	R	15	–52	–28	0.001
Viso	Superior longitudinal fasciculus	R	36	–35	26	0.001
	Middle cerebellar peduncle	–	19	–43	–37	0.002
	Cingulum	R	20	–26	–15	0.002
	Uncinate fasciculus	L	–5	13	–17	0.003
	Posterior limb of internal capsule	L	–21	–16	11	0.003
	Cerebral peduncle	L	–13	–25	–12	0.001
	Cerebral peduncle	R	10	–28	–17	0.001

MCI mild cognitive impairment, *L* left, *R* right, *NDI* neurite density index, *ODI* orientation dispersion index, *Viso* volume fraction of isotropic water molecules, *MNI* Montreal Neurological Institute

longitudinal fasciculus were significantly higher in the AD group (Fig. 1b; Table 3). NDI showed more significant differences between the MCI and AD groups than FA in the same slices of the occipital and parietal lobes (Fig. 1b).

The differences in FA, NDI, ODI, and Viso were greater between the HC and AD groups than between the HC and MCI groups and between the MCI and AD groups (Fig. 1c).

Correlations Between Imaging Parameters and Neuropsychological Scores

No FA values for any fibers were significantly correlated with MMSE and MoCA scores; however, the NDI, ODI, and Viso values of multiple fibers were significantly correlated with MMSE and MoCA scores. The NDI values of the splenium of the corpus callosum ($r=0.633$, $p<0.001$), the ODI value of the left superior longitudinal fasciculus ($r=0.649$, $p<0.001$), and the Viso values of the right cerebral peduncle ($r=-0.508$, $p=0.001$) showed the strongest correlations with MMSE scores. The NDI values of the splenium of the corpus callosum ($r=0.647$, $p<0.001$), the ODI values of the left superior longitudinal fasciculus ($r=0.653$, $p<0.001$), and the Viso values of the left cingulum ($r=-0.505$, $p=0.001$) showed the strongest correlations with the MoCA scores (Fig. 2).

ROC for the Diagnostic Performance

For the diagnosis of MCI, there were no significant differences in the areas under the ROC curves (AUC) between FA and NODDI parameters of the fibers that had been most strongly correlated with neuropsychological testing (Fig. 3). For the diagnosis of AD, when the significance level was considered to be $p<0.05$, the AUC for the NDI value of the splenium of the corpus callosum was larger than the corresponding FA value (AUC = 0.885, 0.714, $p=0.042$). The AUC for the Viso value of the right cerebral peduncle was larger than the corresponding FA value (AUC = 0.934, 0.531, $p=0.004$). The AUC for the left superior longitudinal fasciculus and left cingulum showed no significant differences between FA and NODDI parameters (Fig. 4).

Discussion

This study evaluated the ability of NODDI to detect microstructural white matter changes in MCI and AD by com-

Table 3 White matter structures with reduced NDI and ODI values and increased Viso values in the AD group as compared to the MCI group

Parameters	White matter structures	Side	MNI coordinates			*p*-value
			X	Y	Z	
FA	Superior longitudinal fasciculus	L	–34	–33	35	0.007
	Superior longitudinal fasciculus	R	25	–54	29	0.001
	Corticospinal tract	L	–19	–17	47	0.009
NDI	Superior longitudinal fasciculus	R	44	–48	5	0.004
	Superior longitudinal fasciculus	L	–42	–44	7	0.001
	Cingulum	R	19	–37	–6	0.006
	Uncinate fasciculus	R	14	42	–15	0.006
	External capsule	R	32	6	–10	0.009
	Genu of corpus callosum	–	–3	23	–1	0.005
	Anterior corona radiata	R	64	155	74	0.006
	Anterior corona radiata	L	26	29	2	0.004
	Splenium of corpus callosum	–	–12	–41	10	0.001
	Posterior corona radiata	R	31	–64	19	0.002
	Posterior corona radiata	L	–31	–62	19	0.002
ODI	Superior longitudinal fasciculus	L	–32	–31	25	0.001
	Superior longitudinal fasciculus	R	36	–46	23	0.003
	Cingulum	L	–23	–59	–1	0.005
Viso	Cerebral peduncle	L	–15	–17	–13	0.001
	Corticospinal tract	L	–7	–26	–32	0.001
	Body of corpus callosum	–	–8	–24	25	0.001
	Genu of corpus callosum	–	–13	28	17	0.001
	Superior longitudinal fasciculus	R	49	–41	–10	0.006
	Cerebral peduncle	R	16	–22	–9	0.005
	Corticospinal tract	R	6	–22	–31	0.002
	Cingulum	L	–21	–17	–27	0.001
	External capsule	L	–28	16	–3	0.001

MCI mild cognitive impairment, *AD* Alzheimer's disease, *L* left, *R* right, *NDI* neurite density index, *ODI* orientation dispersion index, *Viso* volume fraction of isotropic water molecules, *MNI* Montreal Neurological Institute, *FA* fractional anisotropy

paring it with conventional DTI. Consistent with previous studies, the FA values of the bilateral cingulum, right superior longitudinal fasciculus, and left posterior limb of the internal capsule decreased significantly in the MCI group if the significance threshold were set at $p<0.05$ [13, 14]; however, with the significance threshold set at $p<0.01$, the results showed that between the HC and MCI groups there were no significant differences in FA, but there were multiple significant differences in NDI and ODI values. Compared with the MCI group, there were more widespread significant differences in NDI than FA in the same slices of the occipital and parietal lobes in the AD group. As shown in Fig. 1a, b, the NDI values of the splenium of the corpus callosum and the bilateral superior longitudinal fasciculus decreased significantly in the MCI and AD groups, whereas the FA values were not significantly different within the same slices. Other studies have also shown that the splenium of the corpus callosum and the superior longitudinal fasciculus exhibit significant reduced FA values at the MCI stage [15, 16]. Some studies indicated that Aβ deposition is one of the AD-related pathological changes and caused cholinergic neurons and axons reduction in the white matter [17, 18], resulting in the reduction of NDI. Overall, the results indicate that NDI values are more sensitive to the changes in white matter than FA which is consistent with a study by Slattery et al. [19]. Furthermore, the regions with significant differences in NDI between MCI and AD groups showed a trend from the lower-middle part of the brain to the upper part of the brain. Thal et al. showed that neurofibrillary tangles (NFT) begin in the transentorhinal region and then spread upward and peripherally to the entorhinal region, the hippocampus and the neocortex [20, 21]. To some extent, the similarity in trends between the present study's NDI values and the spread of NFT may suggest that NDI values correlate with tau protein deposition and some studies have also revealed that NDI values have significant correlations with tau protein deposition [22].

The ODI values were significantly lower mainly in the white matter of the frontal and occipital lobes of the MCI and AD groups compared to the control group. This de-

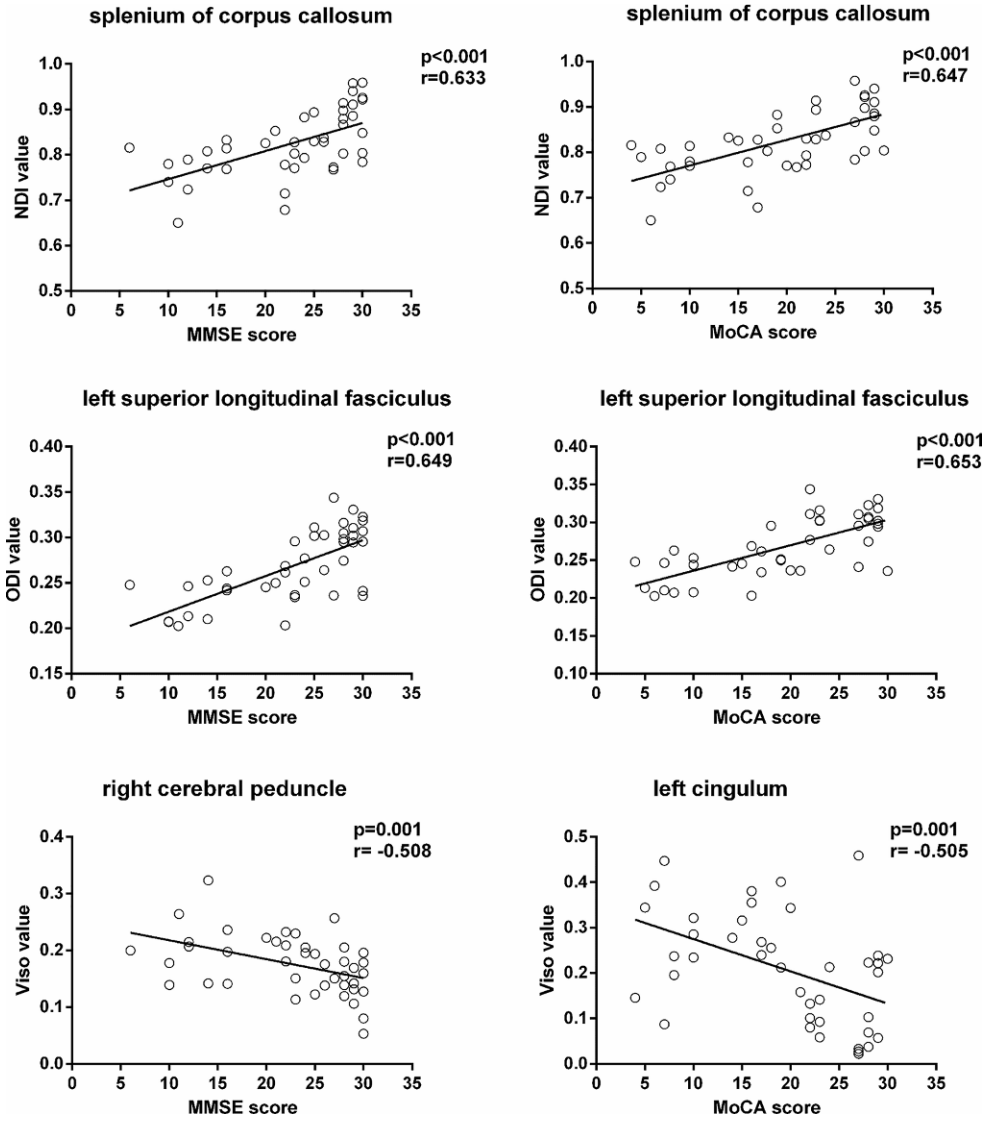

Fig. 2 The correlation analyses with the maximal correlation coefficients between NODDI-derived parameters (NDI, ODI, Viso) and neuropsychological testing scores (*left column* MMSE scores, *right column* MoCA scores). *NODDI* neurite orientation dispersion and density imaging, *FA* fractional anisotropy, *NDI* neurite density index, *ODI* orientation dispersion index, *Viso* volume fraction of isotropic water molecules, *MMSE* mini-mental state examination, *MoCA* Montreal cognitive assessment

crease may be due to that the selectivity of degenerative disorders, which mainly lead to the loss of axons in the secondary fibers in the crossing fibers and leaving more aligned axons in the primary tracts [19].

The Viso values increased in the MCI and AD groups specifically in the brain stem and in the bilateral medial temporal lobes. The increased Viso values were more widespread in the AD group than in the MCI group. Several studies have shown that increased Viso values indicate the degree of atrophy by reflecting cell shrinkage and decreased tissue volume fraction [22, 23]. Therefore, the current study suggests white matter atrophy of medial temporal lobe in MCI and AD, which is consistent with many previous studies that have demonstrated white matter atrophy of medial temporal lobe in the early stage of AD most likely secondary to tau protein deposition [24–27]. The fact that Viso values were already able to detect changes in the MCI group suggest that Viso could be used to monitor progression throughout MCI and AD.

Regarding correlations between NODDI parameters and neuropsychological scores, the NDI values in the splenium of the corpus callosum showed the strongest correlations with MMSE and MoCA scores, which is similar to the result of Wang et al. [15]. This finding is consistent with the hypothesis that NDI values may reflect changes in the number of synapses, which has been shown to correlate with MMSE scores [28, 29]. Additionally, the ODI and Viso values of multiple fibers were significantly correlated with the MMSE and MoCA scores; however, no FA values were correlated with the MMSE and MoCA scores. Furthermore, the AUC of the NDI value of the splenium of corpus callosum and the Viso value of the right cerebral peduncle were significantly larger than the corresponding FA values. These results indicate that NODDI may better

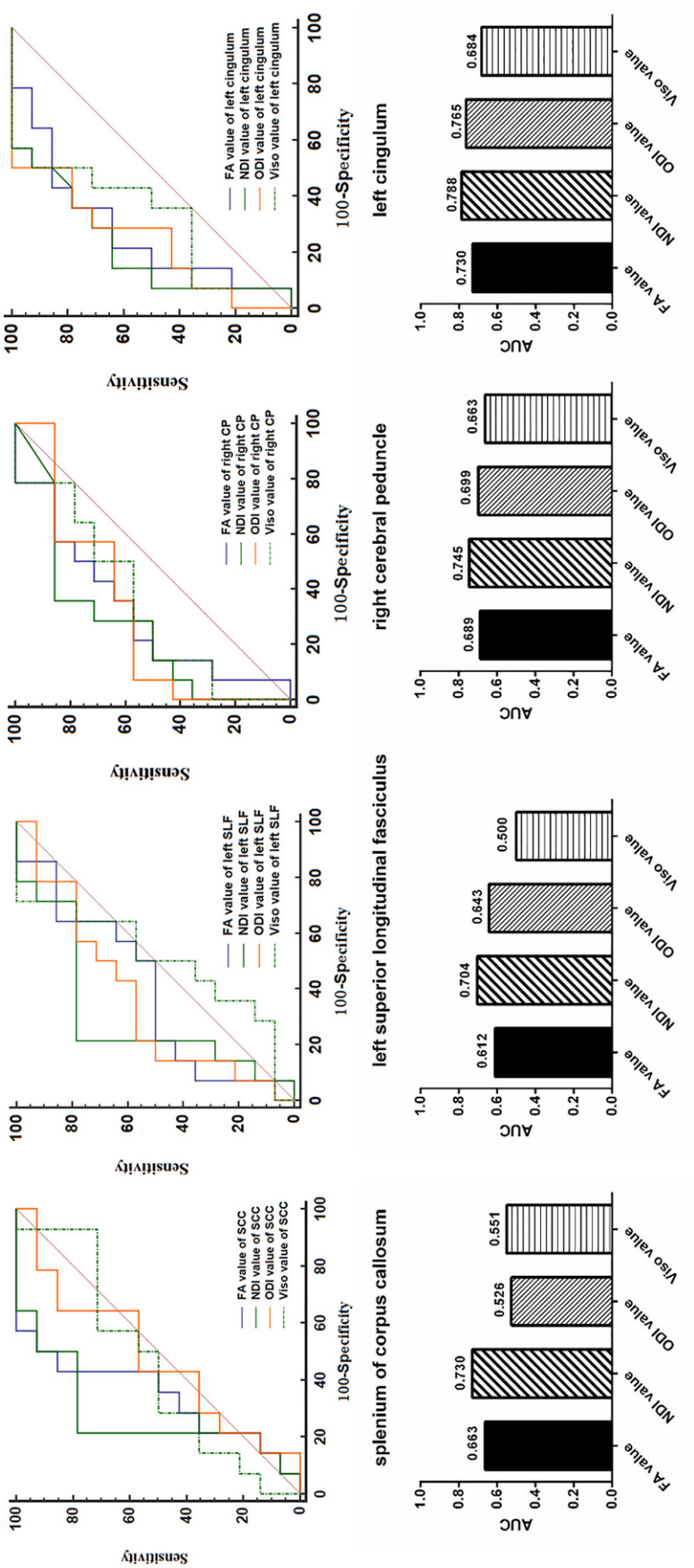

Fig. 3 For the diagnosis of MCI, ROC curve analyses were performed to assess the diagnostic performance of parameters in brain structures with the strongest correlation (*top row*). The AUCs were compared among the different parameters (*bottom row*). There were no significant differences in the AUCs. *MCI* mild cognitive impairment, *SCC* splenium of corpus callosum, *SLF* superior longitudinal fasciculus, *CP* cerebral peduncle, *ROC curve* receiver operating characteristic curve, *AUC* area under the ROC curve, *FA* fractional anisotropy, *NDI* neurite density index, *ODI* orientation dispersion index, *Viso* volume fraction of isotropic water molecules

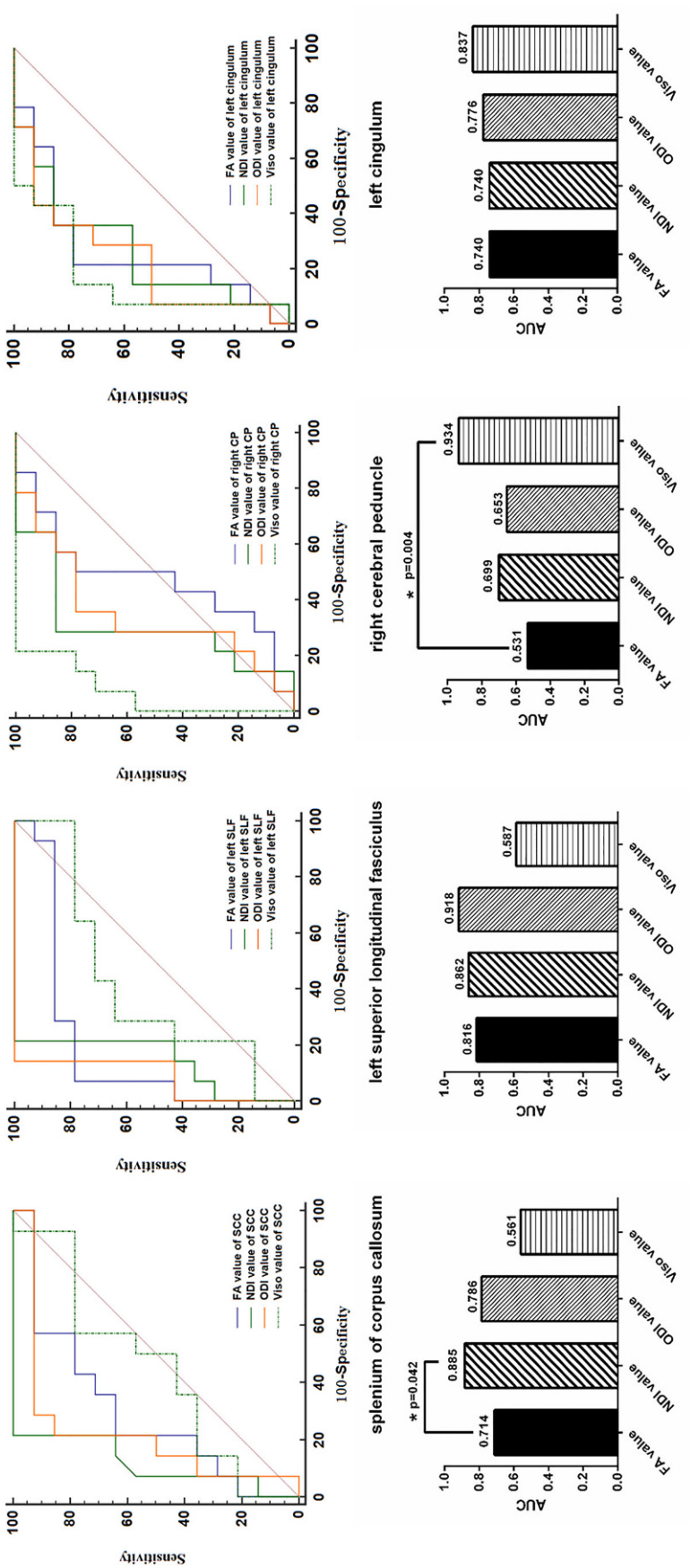

Fig. 4 For the diagnosis of AD, ROC curve analyses were performed to assess the diagnostic performance of parameters in brain structures with the strongest correlation (*top row*). The AUCs were compared among the different parameters (*bottom row*). There were no significant differences in the AUCs. *Asterisk* Significantly different between the two parameters ($p<0.05$). *AD* Alzheimer's disease, *SCC* splenium of corpus callosum, *SLF* superior longitudinal fasciculus, *CP* cerebral peduncle, *ROC curve* receiver operating characteristic curve, *AUC* area under the ROC curve, *FA* fractional anisotropy, *NDI* neurite density index, *ODI* orientation dispersion index, *Viso* volume fraction of isotropic water molecules

reflect clinical cognitive status and may be superior to DTI for diagnosing AD.

There were some limitations in the study. First, the study did not include positron emission tomography (PET) examinations or pathological verification confirming tau protein deposition in the AD and MCI participants involved in this study. Second, the MCI and AD groups were not divided into different subtypes, which relate to different structural damage, degeneration in different regions, and different areas of cognitive impairment. Third, the relatively small sample size limits the accuracy of the results; however, in order to ensure the accuracy of the results, strict inspection of image quality was performed before data processing. Future studies will include CSF biochemical indices and PET examinations, larger samples, and more precise participant subgroups reflecting AD severity.

In conclusion, NDI may be much more sensitive to microstructural white matter alterations in MCI and AD patients. The loss of axons, dendrites and white matter atrophy may be characterized by NODDI in the MCI stage and NODDI could also effectively predict clinical cognitive status and may be superior to DTI in the diagnosis of AD. In brief, NODDI may be a preferable approach for the study of MCI and AD.

Acknowledgements This work was supported by the Natural Scientific Foundation of China (Grant number 30870713, PI: Hongyan Ni) and the Tianjin Natural Science Foundation Project (Grant number 16JCYBJC25900, PI: Hongyan Ni). The authors would like to thank Yuanyuan Chen from the Tianjin International Joint Research Center for Neural Engineering, the Academy of Medical Engineering and Translational Medicine, Tianjin University for assistance in data processing and thank Chunchao Ma from the Department of Neurology, Tianjin First Central Hospital for assistance in providing patients.

Conflict of interest X. Fu, S. Shrestha, M. Sun, Q. Wu, Y. Luo, X. Zhang, J. Yin and H. Ni declare that they have no competing interests.

References

1. Hyman BT, Phelps CH, Beach TG, Bigio EH, Cairns NJ, Carrillo MC, Dickson DW, Duyckaerts C, Frosch MP, Masliah E, Mirra SS, Nelson PT, Schneider JA, Thal DR, Thies B, Trojanowski JQ, Vinters HV, Montine TJ. National Institute on Aging-Alzheimer's Association guidelines for the neuropathologic assessment of Alzheimer's disease. Alzheimers Dement. 2012;8:1–13.
2. Radanovic M, Pereira FR, Stella F, Aprahamian I, Ferreira LK, Forlenza OV, Busatto GF. White matter abnormalities associated with Alzheimer's disease and mild cognitive impairment: a critical review of MRI studies. Expert Rev Neurother. 2013;13:483–93.
3. Amlien IK, Fjell AM. Diffusion tensor imaging of white matter degeneration in Alzheimer's disease and mild cognitive impairment. Neuroscience. 2014;276:206–15.
4. Mitchell AJ, Shiri-Feshki M. Rate of progression of mild cognitive impairment to dementia—meta-analysis of 41 robust inception cohort studies. Acta Psychiatr Scand. 2009;119:252–65.
5. Jones DK, Knösche TR, Turner R. White matter integrity, fiber count, and other fallacies: the do's and don'ts of diffusion MRI. Neuroimage. 2013;73:239–54.
6. Zhang H, Schneider T, Wheeler-Kingshott CA, Alexander DC. NODDI: practical in vivo neurite orientation dispersion and density imaging of the human brain. Neuroimage. 2012;61:1000–16.
7. Merluzzi AP, Dean DC, Adluru N, Suryawanshi GS, Okonkwo OC, Oh JM, Hermann BP, Sager MA, Asthana S, Zhang H, Johnson SC, Alexander AL, Bendlin BB. Age-dependent differences in brain tissue microstructure assessed with neurite orientation dispersion and density imaging. Neurobiol Aging. 2016;43:79–88.
8. Sepehrband F, Clark KA, Ullmann JF, Kurniawan ND, Leanage G, Reutens DC, Yang Z. Brain tissue compartment density estimated using diffusion-weighted MRI yields tissue parameters consistent with histology. Hum Brain Mapp. 2015;36:3687–702.
9. Grussu F, Schneider T, Tur C, Yates RL, Tachrount M, Ianuş A, Yiannakas MC, Newcombe J, Zhang H, Alexander DC, DeLuca GC, Gandini Wheeler-Kingshott CAM. Neurite dispersion: a new marker of multiple sclerosis spinal cord pathology? Ann Clin Transl Neurol. 2017;4:663–79.
10. Jespersen SN, Bjarkam CR, Nyengaard JR, Chakravarty MM, Hansen B, Vosegaard T, Ostergaard L, Yablonskiy D, Nielsen NC, Vestergaard-Poulsen P. Neurite density from magnetic resonance diffusion measurements at ultrahigh field: comparison with light microscopy and electron microscopy. Neuroimage. 2010;49:205–16.
11. Petersen RC. Mild cognitive impairment as a diagnostic entity. J Intern Med. 2004;256:183–94.
12. Albert MS, DeKosky ST, Dickson D, Dubois B, Feldman HH, Fox NC, Gamst A, Holtzman DM, Jagust WJ, Petersen RC, Snyder PJ, Carrillo MC, Thies B, Phelps CH. The diagnosis of mild cognitive impairment due to Alzheimer's disease: recommendations from the National Institute on Aging-Alzheimer's Association workgroups on diagnostic guidelines for Alzheimer's disease. Alzheimers Dement. 2011;7:270–9.
13. Liu Y, Spulber G, Lehtimäki KK, Könönen M, Hallikainen I, Gröhn H, Kivipelto M, Hallikainen M, Vanninen R, Soininen H. Diffusion tensor imaging and tract-based spatial statistics in Alzheimer's disease and mild cognitive impairment. Neurobiol Aging. 2011;32:1558–71.
14. Sexton CE, Kalu UG, Filippini N, Mackay CE, Ebmeier KP. A meta-analysis of diffusion tensor imaging in mild cognitive impairment and Alzheimer's disease. Neurobiol Aging. 2011;32:2322.e5–e18.
15. Wang PN, Chou KH, Chang NJ, Lin KN, Chen WT, Lan GY, Lin CP, Lirng JF. Callosal degeneration topographically correlated with cognitive function in amnestic mild cognitive impairment and Alzheimer's disease dementia. Hum Brain Mapp. 2014;35:1529–43.
16. Liu J, Liang P, Yin L, Shu N, Zhao T, Xing Y, Li F, Zhao Z, Li K, Han Y. White matter abnormalities in two different subtypes of amnestic mild cognitive impairment. PLoS ONE. 2017;12:e170185.
17. Bellucci A, Luccarini I, Scali C, Prosperi C, Giovannini MG, Pepeu G, Casamenti F. Cholinergic dysfunction, neuronal damage and axonal loss in TgCRND8 mice. Neurobiol Dis. 2006;23:260–72.
18. Sun SW, Liang HF, Mei J, Xu D, Shi WX. In vivo diffusion tensor imaging of amyloid-beta-induced white matter damage in mice. J Alzheimers Dis. 2014;38:93–101.
19. Slattery CF, Zhang J, Paterson RW, Foulkes AJM, Carton A, Macpherson K, Mancini L, Thomas DL, Modat M, Toussaint N, Cash DM, Thornton JS, Henley SMD, Crutch SJ, Alexander DC, Ourselin S, Fox NC, Zhang H, Schott JM. ApoE influences regional white-matter axonal density loss in Alzheimer's disease. Neurobiol Aging. 2017;57:8–17.

20. Thal DR, Attems J, Ewers M. Spreading of amyloid, tau, and microvascular pathology in Alzheimer's disease: findings from neuropathological and neuroimaging studies. J Alzheimers Dis. 2014;42 Suppl 4:S421-9.
21. Calderon-Garcidueñas AL, Duyckaerts C. Alzheimer disease. Handb Clin Neurol. 2017;145:325–37.
22. Colgan N, Siow B, O'Callaghan JM, Harrison IF, Wells JA, Holmes HE, Ismail O, Richardson S, Alexander DC, Collins EC, Fisher EM, Johnson R, Schwarz AJ, Ahmed Z, O'Neill MJ, Murray TK, Zhang H, Lythgoe MF. Application of neurite orientation dispersion and density imaging (NODDI) to a tau pathology model of Alzheimer's disease. Neuroimage. 2016;125:739–44.
23. Merluzzi AP, Dean DC 3rd, Adluru N, Suryawanshi GS, Okonkwo OC, Oh JM, Hermann BP, Sager MA, Asthana S, Zhang H, Johnson SC, Alexander AL, Bendlin BB. Age-dependent differences in brain tissue microstructure assessed with neurite orientation dispersion and density imaging. Neurobiol Aging. 2016;43:79–88.
24. Li J, Pan P, Huang R, Shang H. A meta-analysis of voxel-based morphometry studies of white matter volume alterations in Alzheimer's disease. Neurosci Biobehav Rev. 2012;36:757–63.
25. Pettigrew C, Soldan A, Sloane K, Cai Q, Wang J, Wang MC, Moghekar A, Miller MI, Albert M; BIOCARD Research Team. Progressive medial temporal lobe atrophy during preclinical Alzheimer's disease. Neuroimage Clin. 2017;16:439–46.
26. Mormino EC, Papp KV. Amyloid accumulation and cognitive decline in clinically normal older individuals: implications for aging and early alzheimer's disease. J Alzheimers Dis. 2018;64(s1): S633–46.
27. Mito R, Raffelt D, Dhollander T, Vaughan DN, Tournier JD, Salvado O, Brodtmann A, Rowe CC, Villemagne VL, Connelly A. Reply: Cortical tau pathology: a major player in fibre-specific white matter reductions in Alzheimer's disease? Brain. 2018;141:e45.
28. Scheff SW, Price DA, Schmitt FA, Scheff MA, Mufson EJ. Synaptic loss in the inferior temporal gyrus in mild cognitive impairment and Alzheimer's disease. J Alzheimers Dis. 2011;24:547–57.
29. Scheff SW, Price DA, Schmitt FA, Mufson EJ. Hippocampal synaptic loss in early Alzheimer's disease and mild cognitive impairment. Neurobiol Aging. 2006;27:1372–84.